Journal of Dental Sciences (2021) 16, 628–635

Available online at www.sciencedirect.com

ScienceDirect

journal homepage: www.e-jds.com

Original Article

# Strain analysis of anterior resin-bonded fixed dental prostheses with different thicknesses of high translucent zirconia

Michiko Noda [a], Satoshi Omori [a*], Reina Nemoto [a], Erika Sukumoda [a], Mina Takita [a], Richard Foxton [b], Kosuke Nozaki [a], Hiroyuki Miura [a]

[a] *Department of Fixed Prosthodontics, Division of Oral Health Sciences, Graduate School of Medical and Dental Sciences, Tokyo Medical and Dental University (TMDU), Tokyo, Japan*
[b] *Restorative Dentistry, Faculty of Dentistry, Oral & Craniofacial Sciences, King's College London, London, UK*

Received 2 September 2020; Final revision received 7 October 2020
Available online 23 October 2020

**KEYWORDS**
Anterior restoration;
High translucent zirconia;
Resin-bonded fixed dental prostheses;
Retainer thickness;
Strain analysis

**Abstract** *Background/purpose:* High translucent zirconia has been used as a new monolithic zirconia prosthesis, which has the potential to make anterior resin-bonded fixed dental prostheses (RBFDPs) without veneering porcelain. However, it is unclear whether the RBFDPs retainer can be thinned as much as conventional zirconia RBFDPs. The aim of this study was to assess the usability of high translucent zirconia RBFDPs with a thin retainer thickness by evaluating differences in retainer thickness on the surface strain.
*Materials and methods:* A model with a missing upper lateral incisor was used. The abutment teeth were upper central incisor and canine. Three types of RBFDPs were fabricated as follows: metal RBFDPs with a retainer thickness of 0.8 mm (0.8M), and high translucent zirconia RBFDPs with a retainer thicknesses of 0.8 and 0.5 mm (0.8Z, 0.5Z) (n = 10). The fitness of the margins was evaluated by the silicone replica technique. The surface strain of each retainer under static loading was measured and statistically analyzed using a t-test with Bonferroni correction.
*Results:* The marginal fitness of all RBFDPs was under 76.1 μm, which was clinically acceptable. Each strain of the 0.8Z and 0.5Z groups was significantly lower than that of the 0.8M ($p < 0.05$). There was no difference in strain of the zirconia RBFDPs even if the retainer thickness was changed.
*Conclusion:* Our results suggest that the high translucent zirconia RBFDPs can be manufactured with a retainer thickness of 0.5 mm, which reduces the amount of tooth preparation compared to the metal RBFDPs.

* Corresponding author. Department of Fixed Prosthodontics, Division of Oral Health Sciences, Graduate School of Medical and Dental Sciences, Tokyo Medical and Dental University (TMDU), 1-5-45 Yushima, Bunkyo-ku, Tokyo, 113-8549, Japan. Fax: +81-3-5803-0201.
*E-mail address:* s.omori.fpro@tmd.ac.jp (S. Omori).

https://doi.org/10.1016/j.jds.2020.10.002

## Introduction

Resin-bonded fixed dental prostheses (RBFDPs) are widely used in clinics because the procedure requires less tooth reduction than conventional fixed dental prostheses (FDPs). Among the varieties of materials for RBFDPs, much attention has been paid to yttria-stabilized tetragonal zirconia polycrystal because of its high mechanical strength and esthetics.[1–4] Using conventional zirconia as a framework for RBFDPs, zirconia RBFDPs can be made with thinner retainers (0.5 mm) compared to the retainer thickness of traditional metal RBFDPs (0.8 mm).[5–7] The advantage of using zirconia is that tooth reduction can be minimized.[5,6] Zirconia RBFDPs have also been reported to have better survival rates than traditional metal RBFDPs.[8,9]

Conventional zirconia RBFDPs, however, require a veneering porcelain on the labial surface. The most frequent clinical complication with zirconia FDPs is chipping of the veneering porcelain.[9,10] This is more likely to occur with zirconia FDPs than metal FDPs.[11] Although finite element analysis has helped elucidate the optimum design for the zirconia framework in order to minimise porcelain chipping,[12] a monolithic prosthesis would reduce complications such as chipping and fracture.[13]

Recently, highly translucent zirconia has been developed to fabricate single and multiple prostheses with improved tooth-color matching.[14,15] One benefit of high translucency is better replication of tooth color and therefore monolithic translucent zirconia FDPs may be a satisfactory option as esthetic prostheses with monolayer structures.[16,17] Translucent zirconia restorations can be strongly bonded by sandblasting with alumina and selecting an adhesive resin cement as with conventional zirconia.[18] Moreover, tooth preparation for RBFDPs should be limited within enamel as much as possible.[19,20] Hence, high translucent zirconia has the potential for fabricating RBFDPs with thin retainers while maintaining rigidity and preserving abutment tooth structure. However to date, there has been no research published, which has investigated the use of high translucent zirconia for anterior RBFDPs and the effect of retainer thickness on the surface strain. The aim of this study therefore was to assess the suitability of high translucent zirconia RBFDPs with a thin retainer thickness by evaluating different retainer thicknesses (0.8 mm, 0.5 mm) on surface strain using the strain gage method and comparing with metal RBFDPs.

## Materials and methods

### Fabrication of master die

A jaw model with a missing upper right lateral incisor (D51FE-500 A-QF, Nissin Dental Product Inc., Kyoto, Japan) was used as the experimental model. The upper right central incisor and canine were prepared for RBFDPs as abutment teeth. The palatal surface of each abutment was reduced by 0.5 mm. A hole with a diameter of 1.0 mm and a depth of 0.5 mm was formed on the palatal surface. A groove with a length of 2.0 mm and a depth of 0.5 mm was formed on each side of the proximal surface. The cervical finishing line was prepared as a chamfer. All axiogingival internal line angles were rounded off (Fig. 1).[5]

After taking an impression of the jaw model with silicone impression material (Examixfine, GC Corp., Tokyo, Japan), a metal teeth model of the same shape was fabricated using a cobalt chromium alloy (Cobaltan clasp, Shofu Inc., Kyoto, Japan). This metal model was used as the master die.

The master die was fixed to an aluminum tube (20.0 mm length and diameter and 1.0 mm thickness) with self-curing acrylic resin (Unifast III, GC Corp.). The axial inclination of the abutments was 45° from the long axis of the abutment teeth.

### Fabrication of RBFDPs

An impression of the master die was obtained using hydrophilic vinyl polysiloxane impression materials (FusionII wash type and monophase type, GC Corp.). The impressions were poured with type IV die stone (New Fujirock, GC Corp.). Using this stone die, three groups of RBFDPs (n = 10 each) were fabricated as follows:

- Metal RBFDPs with a retainer thickness of 0.8 mm (0.8M).
- High translucent zirconia RBFDPs with a retainer thickness of 0.8 mm (0.8Z).
- High translucent zirconia RBFDPs with a retainer thickness of 0.5 mm (0.5Z).

### Fabrication of high translucent zirconia RBFDPs

The stone die was scanned using a dental scanner (Lava Scan, 3 M Deutschland GmbH, Seefeld, Germany) to fabricate translucent zirconia RBFDPs. All parts of the RBFDPs were designed using CAD software (DWOS LAVA edition, Dental Wings, Montreal, Canada). Each cross-sectional area between the canine and pontic was 11.0 $mm^2$ (0.8Z), 11.0 $mm^2$ (0.5Z), and the cross-sectional area between the central incisor and pontic was 11.1 $mm^2$ (0.8Z), 10.1 $mm^2$ (0.5Z). Translucent zirconia discs (3 M Lava Esthetic Fluorescent Full-Contour Zirconia, 3 M Deutschland GmbH) were milled on a milling machine (DWX-52DC, Roland DG Corp., Shizuoka, Japan) and sintered. Only the labial surfaces of the translucent zirconia RBFDPs were glazed with glaze paste (Initial IQ Lustre Pastes, GC Corp.) and sintered once at 800 °C. All specimens were adjusted to fit the master die, and all surfaces except for the bonding surface were polished. Ten specimens each were fabricated for 0.8Z and 0.5Z.

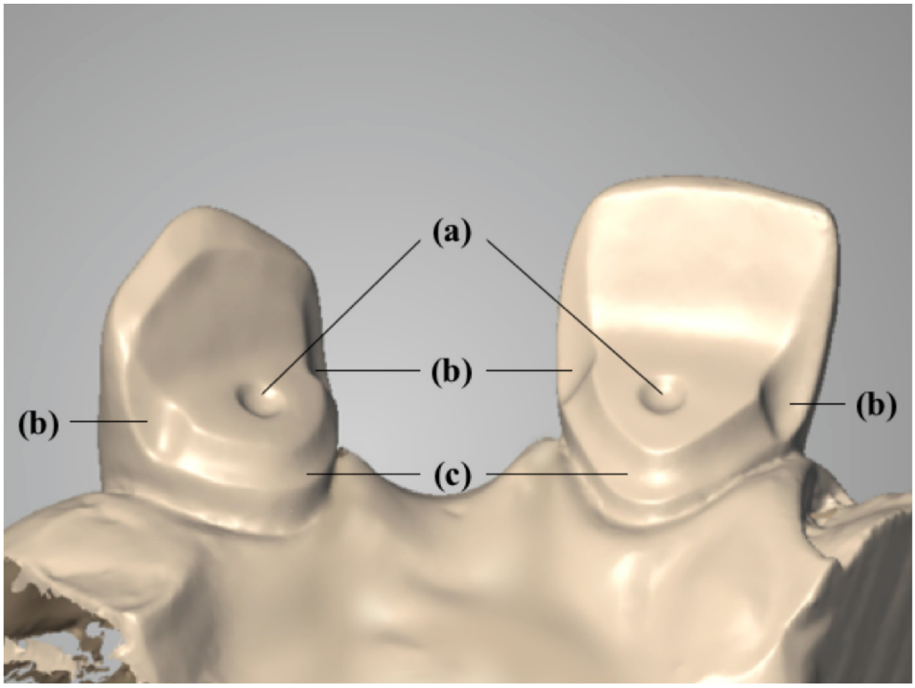


**Figure 1** Tooth preparation image. (a) Hole with a diameter of 1.0 mm and a depth of 0.5 mm. (b) Groove with a length of 2.0 mm and a depth of 0.5 mm. (c) Cervical chamfer.

## Fabrication of metal RBFDPs

High translucent zirconia RBFDP (0.8Z) was duplicated as a resin pattern (Pattern resin XF, GC Corp.) for metal RBFDPs (0.8M). A line 1.0 mm inside the outline of the pontic was defined as the cut-back margin, and the labial surface of the pontic was reduced by 1.0 mm for the veneering composite resin. Retention beads (Retention beads II set SSS, GC Corp.) were attached to the bottom of the cut-back area. The patterns were cast with gold-silver palladium alloy (Castwell M.C. 12% Gold, GC Corp.), and the cut-back part facing the composite resin was then veneered (Pearleste, Tokuyama Dental Corp., Tokyo, Japan). Finally, the metal RBFDPs were adjusted and polished to fit the master die. Ten specimens were fabricated for 0.8M.

## Marginal fitting test

All RBFDPs were checked for marginal fit with the master die using black silicone (Bite Checker, GC Corp.). Then, cross-sections of the black silicone were measured using the micron depth and a height measuring machine (Micron Depth & Height Measuring Scope Model KY-60, Nissho Optical Co., Saitama, Japan) at four regions (incisal, mesial, distal, and cervical margin).

## Cementation

The bonding surfaces of the retainers of the RBFDPs were abraded with 70 μm $Al_2O_3$ airborne particles (0.2 MPa for 10 s at a distance of 10 mm) and ultrasonically cleaned in distilled water for 10 min. The bonding surfaces of the master die were cleaned with alcohol, and a primer (Panavia V5 Tooth Primer, Kuraray Noritake Dental Inc., Tokyo, Japan) was applied. The cohesive surfaces of the RBFDPs were cleaned with alcohol, and a ceramic primer (Clearfil Ceramic Primer Plus, Kuraray Noritake Dental Inc.) was applied. The RBFDPs were cemented to the master die with resin cement (Panavia V5, Kuraray Noritake Dental Inc.) according to the instructions from the manufacturer.

## Measurement of strain

Two triaxial stacked rosette gages (Rosette Gage KFG-1-120-D17-11N30C2, Kyowa Electronic Instruments Co., LTD., Tokyo, Japan) were attached to the palatal surface of each retainer with strain gage cement (cc33 A, Kyowa Electronic Instruments Co., Ltd.) using finger pressure for 1 min (Fig. 2). These specimens were stored at room temperature for 24 h and fixed in position using a jig.

Using a universal testing machine (Autograph AGS-H, Shimadzu Corp., Tokyo, Japan), the specimens were loaded with a cross-head speed of 1.0 mm/min up to 200 N using a stainless-steel rod with a 4 mm diameter ball end.[5,6,21] The loading direction was 45° to the long axis of the abutment teeth,[22] and the load was applied to the center of the pontic (Figs. 3 and 4).[5,6] The outputs from the strain gages were recorded using a software (DCS-100 A, Kyowa Electronic Instruments Co., LTD.) via a sensor interface (300 B, Kyowa Electronic Instruments Co., LTD.). Then, the maximum principal strain ($\varepsilon_{max}$) [με] was calculated as follows:

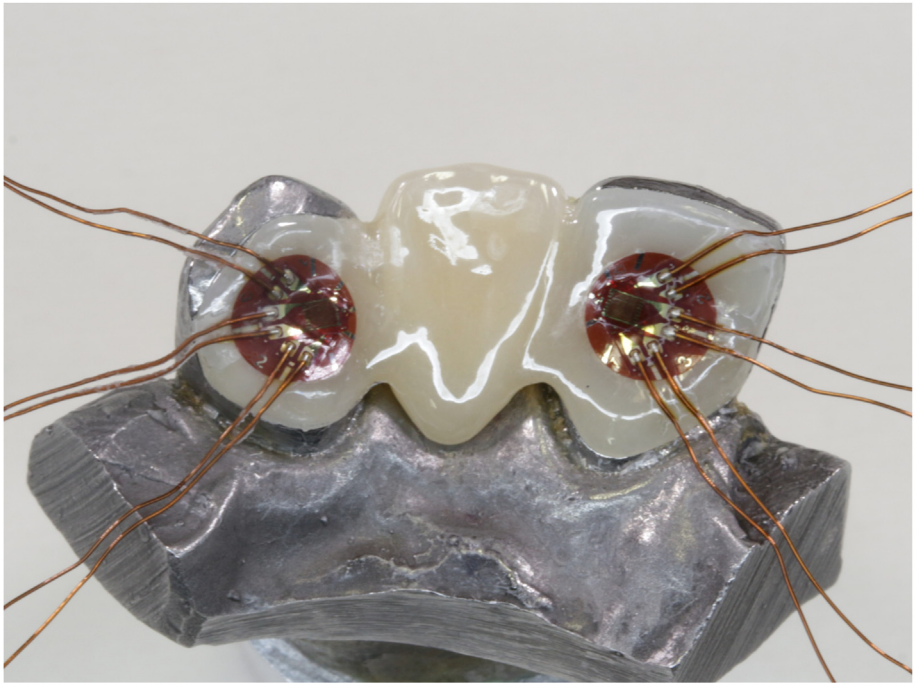

**Figure 2** Strain gages on each retainer.

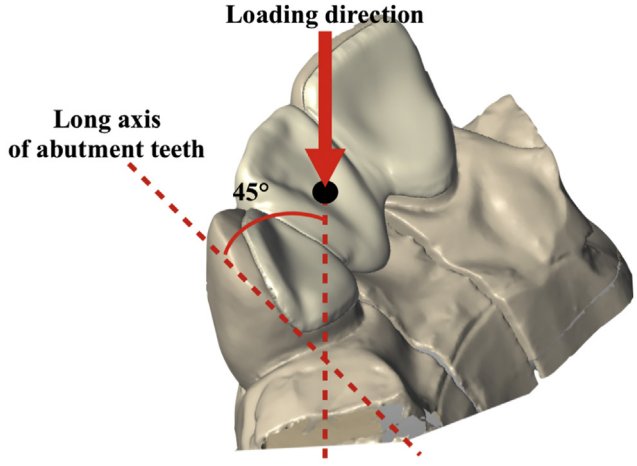


**Figure 3** Loading direction and location. The loading direction was at 45° to the long axis of the abutment teeth, and the load was applied onto the center of the pontic.

$$\varepsilon_{max} = \frac{1}{2}(\varepsilon_a + \varepsilon_c) + \frac{1}{2}\sqrt{(\varepsilon_a - \varepsilon_c)^2 + (2\varepsilon_b - \varepsilon_a - \varepsilon_c)^2} \quad (1)$$

where $\varepsilon_a$, $\varepsilon_b$, and $\varepsilon_c$ are the strains of each gage component. This strain gage was composed of three liner gages placed at the 0°, 45°, and 90° positions (Figs. 2 and 5). Positive values indicate tensile strain, and negative values indicate compressive strain. The direction of the maximum principal strain, which is denoted by the angle $\theta$ from the axis $\varepsilon_a$, can be calculated as follows:

$$\theta = \frac{1}{2}\tan^{-1}\left(\frac{2\varepsilon_b - \varepsilon_a - \varepsilon_c}{\varepsilon_a - \varepsilon_c}\right) \quad (2)$$

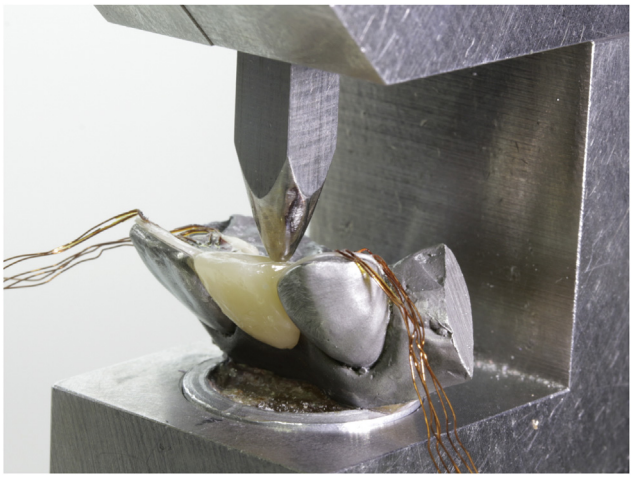

**Figure 4** Photograph of loading being applied to the pontic. The specimens were loaded with a cross-head speed of 1.0 mm/min up to 200 N using a stainless-steel rod with a 4 mm diameter ball end.

## Statistical analyses

Statistical analysis was performed using statistical software (SPSS 22.0, SPSS Inc., Chicago, IL, USA). After confirming the normality of the data using the Shapiro–Wilk test, the difference in $\varepsilon_{max}$ between each group was calculated using a t-test with Bonferroni correction. In the same way, the difference in $\theta$ was also analyzed. A significant difference was observed when $p < 0.05$.

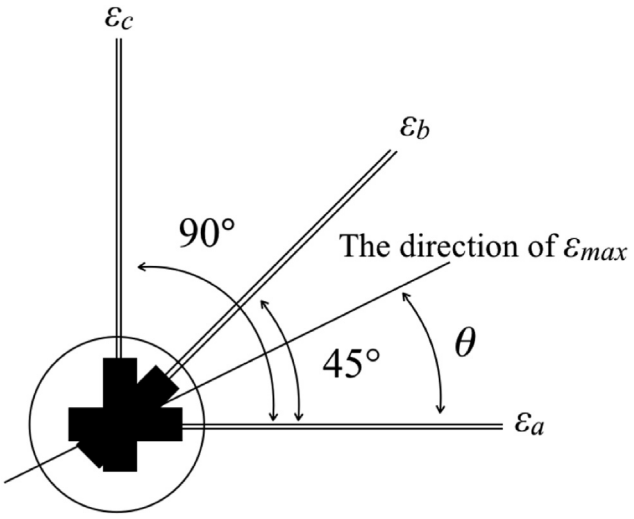


**Figure 5** The direction of maximum principal strain ($\varepsilon_{max}$) and each components of strain gage. Three liner gages were placed at 0°, 45°, and 90° positions. The direction of $\varepsilon_{max}$ is denoted by the angle $\theta$ from the axis $\varepsilon_a$.

## Results

The results of the marginal fitting test are shown in Table 1. The silicone replica between the abutment teeth and RBFDPs was smooth and constant. The maximum value of the mean marginal gaps was 76.1 μm.

The directions of maximum principle strain are shown in Table 2. All groups appeared to be nearly the same in each type of abutment (Fig. 7). The retainers on the canine and central incisors were distorted in the buccopalatal direction. There was no significant difference among the mean values of $\theta$ for each group ($p > 0.05$).

The mean values of the maximum principle strain are shown in Fig. 6. The maximum principle strain of 0.8M in the canine was greater than that of 0.8Z and 0.5Z ($p < 0.001$). However, there was no significant difference in the strain between 0.8Z and 0.5Z. The maximum principle strain of 0.8M in the central incisor was greater than that of 0.8Z ($p = 0.011$) and 0.5Z ($p = 0.020$). However, there was no significant difference in the strain between 0.8Z and 0.5Z (Fig. 6).

## Discussion

While there have been a number of studies on fracture resistance and characteristics of RBFDPs,[22–25] there have been few studies on the strain of RBFDPs using the strain gage method. In a previous study, the strain gage method was used to analyze the surface strain or deformation of prostheses.[5,6] Due to the deformation, the stress will concentrate on the resin cement layer, and prostheses will debond.[26,27] Using the strain gage method, this deformation can be measured with a high sensitivity.[28] This method can also measure the real strain on dental restorations in the oral cavity. In another previous study, there was no significant difference in strain between the in vivo and in vitro models.[29] In other words, the strain gage method used in vitro, can provide clinically useful information. The present study mimicked the clinical situation by designing the shape of RBFDPs to anatomical form and the marginal gap of RBFDPs was well under 120 μm, a value, which is clinically acceptable.[30] In order to measure the strain under severe conditions, a force of 200 N was applied to the center of the pontic assuming a maximum occlusal force (210.5 N) from an angle of 45° to the long axis of the abutment teeth.[21,22] One metal (cobalt-chromium alloy) model was selected and artificial periodontal ligaments were not used in order to eliminate all other factors except the difference of the RBFDPs.

**Table 1** Results of marginal fitting test [μm].

| | canine | | | | central incisor | | | |
|---|---|---|---|---|---|---|---|---|
| Region | M | D | I | C | M | D | I | C |
| 0.8M | 59.5 | 58.8 | 76.1 | 55.3 | 72.2 | 56.7 | 52.5 | 65.2 |
| 0.8Z | 45.7 | 50.4 | 51.4 | 62.7 | 57.0 | 61.8 | 63.8 | 61.0 |
| 0.5Z | 42.8 | 53.6 | 38.5 | 66.4 | 42.3 | 53.7 | 51.2 | 46.6 |

"C" represents cervical margin, "D" represents distal margin, "I" represents incisal margin, and "M" represents mesial margin.

Deformation of prostheses is determined by the moment of force and the elastic modulus. The reason why the surface strain of metal RBFDPs (0.8M) was larger than that of high translucent zirconia RBFDPs (0.8Z) even with the same retainer thickness was considered to be due to the difference in elastic modulus. It is reported that the elastic modulus of gold-silver-palladium alloy is 86 GPa,[31] and that of high translucent zirconia is 200–210 GPa.[15] Since high translucent zirconia has high rigidity, it is less likely to be distorted. This result suggested that high translucent zirconia might be more suitable for RBFDPs than metal. In addition, the thin high translucent zirconia RBFDPs (0.5Z) were less likely to be distorted than metal RBFDPs (0.8M) and the strain of high translucent zirconia RBFDPs showed no difference even if the retainer thickness was changed (0.8Z and 0.5Z). These facts showed that high translucent zirconia RBFDPs can be made with a retainer thickness of 0.5 mm as well as conventional zirconia.[5] These findings are very important from the point of minimal intervention and preservation of tooth structure. The thickness of the frameworks of metal RBFDPs generally must be 0.7 mm or more.[7] However, it has been reported that the palatal enamel thickness of the teeth of Japanese people was 0.3–0.6 mm in the upper central incisor and 0.4–0.9 mm in the upper canine.[32] Brokos et al. concluded that the palatal enamel thickness of the upper anterior teeth is 0.7 mm and the palatal area is the thinnest area.[33] Therefore, it can be argued that high translucent zirconia is superior to metal because the tooth preparation area can be kept within enamel using this type of zirconia.

To prevent debonding of RBFDPs, it has been reported that preparing a groove on the abutment teeth and increasing the bonding surface area are beneficial.[5,34,35] Based on this mechanism, it can be suggested that the strain of central incisor was smaller than that of canine because the central incisor had a larger surface area than the canine. In addition, there are also some reports

**Table 2** Mean values of $\theta$.

| Experimental group | 0.8M | | 0.8Z | | 0.5Z | |
|---|---|---|---|---|---|---|
| | canine | central incisor | canine | central incisor | canine | central incisor |
| Mean values of $\theta$ [°] | 0.2 | 89.8 | 0.2 | 89.8 | 0.2 | 89.7 |
| (SD) | (0.12) | (0.13) | (0.10) | (0.12) | (0.22) | (0.08) |

"$\theta$" is the angle from the axis $\varepsilon_a$ and represents the direction of maximum principal strain.

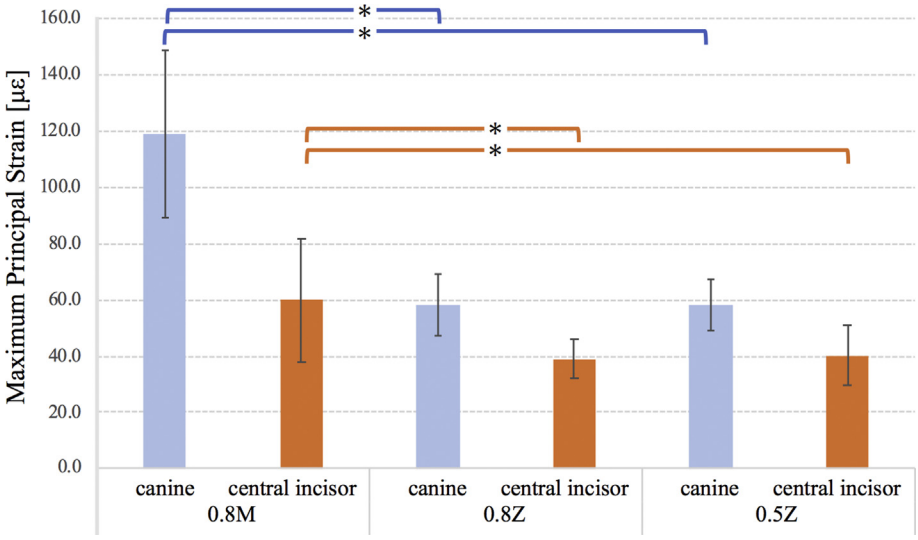


**Figure 6** Maximum principal strain ($\varepsilon_{max}$) [με] (*: $p < 0.05$).

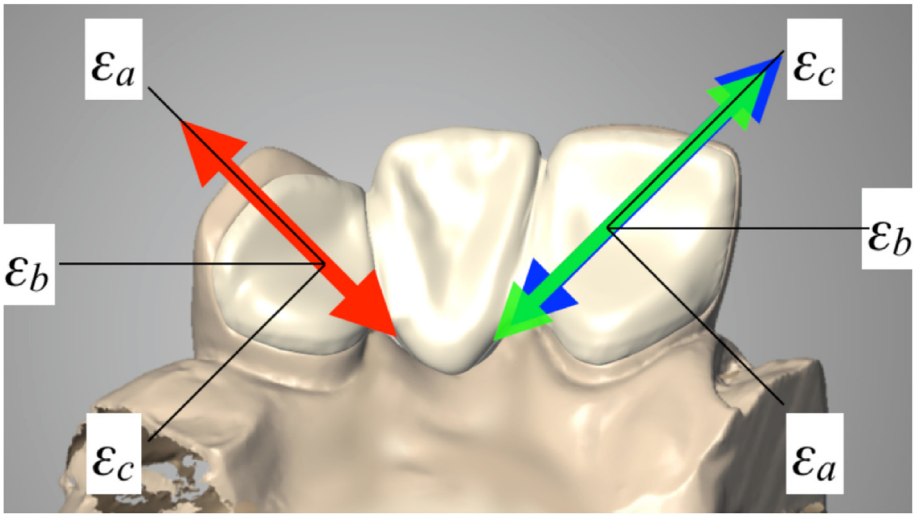


**Figure 7** Direction of $\varepsilon_{max}$ for each group. Red arrow represents direction in canine for 0.8M, 0.8Z, and 0.5Z. Blue arrow represents direction in central incisor for 0.8M and 0.8Z. Green arrow represents direction in central incisor of 0.5Z. (For interpretation of the references to color in this figure legend, the reader is referred to the Web version of this article).

indicating that as the cross-sectional area of the connector increases, the fracture load of prostheses increases.[36,37] In this study, proximal grooves were prepared and the RBFDPs were fabricated with monolithic zirconia. Preparing proximal grooves leads to an increase in both the bonding surface area and cross-sectional area of the connector. The monolithic RBFDPs do not require the connector to be cut back for veneering porcelain, which means the cross-sectional area of the connector is maintained. The cross-sectional area between the canine and pontic was 11.0 $mm^2$ (0.8Z), 11.0 $mm^2$ (0.5Z), and the cross-sectional area between the central incisor and pontic was 11.1 $mm^2$

(0.8Z), 10.1 $mm^2$ (0.5Z). Each cross-sectional area was approximately equal and sufficient for retention of the prostheses.[36,37] Therefore, it was considered that there was no difference in strain between 0.8Z and 0.5Z. These results suggested that the RBFDPs connector where stress concentrates most during functioning can be composed of only zirconia with high rigidity, which may reduce the risk of debonding.

This study revealed that the maximum principle strain of the retainer under simulated occlusal force was reduced using high translucent zirconia RBFDPs compared to traditional metal RBFDPs. The translucent zirconia enabled the reduction of retainer thickness from the traditional 0.8 mm—0.5 mm, which minimizes the amount of tooth preparation and establishes enamel-zirconia adhesion. The behavior of translucent zirconia RBFDPs may contribute to the development of long-term functioning dental prostheses.

## Declaration of competing interest

The authors have no conflicts of interest relevant to this article.

## Acknowledgements

This study was partly supported by Grants-in-Aid for Scientific Research (JSPS KAKENHI Grant Number JP18K17113) from Japan Society for the Promotion of Science.

## References

1. Stylianou A, Liu PR, O'Neal SJ, Essig ME. Restoring congenitally missing maxillary lateral incisors using zirconia-based resin bonded prostheses. *J Esthetic Restor Dent* 2016;28:8—17.
2. Vasques WF, Martins FV, Magalhães JC, Fonseca EM. A low cost minimally invasive adhesive alternative for maxillary central incisor replacement. *J Esthetic Restor Dent* 2018;30:469—73.
3. Sasse M, Kern M. CAD/CAM single retainer zirconia-ceramic resin-bonded fixed dental prostheses: clinical outcome after 5 years. *Int J Comput Dent* 2013;16:109—18.
4. Sasse M, Eschbach S, Kern M. Randomized clinical trial on single retainer all-ceramic resin-bonded fixed partial dentures: influence of the bonding system after up to 55 months. *J Dent* 2012;40:783—6.
5. Nemoto R, Nozaki K, Fukui Y, Yamashita K, Miura H. Effect of framework design on the surface strain of zirconia fixed partial dentures. *Dent Mater J* 2013;32:289—95.
6. Matsukawa K, Nemoto R, Nozaki K, et al. The influence of the framework thickness on surface strain of the 3-unit zirconia resin-bonded fixed dental prostheses under the functional loading. *Asian Pac J Dent* 2017;17:1—7.
7. Ibbetson R. Clinical considerations for adhesive bridgework. *Dent Update* 2004;31:254—60.
8. Alraheam IA, Ngoc CN, Wiesen CA, Donovan TE. Five-year success rate of resin-bonded fixed partial dentures: a systematic review. *J Esthetic Restor Dent* 2019;31:40—50.
9. Thoma DS, Sailer I, Ioannidis A, Zwahlen M, Makarov N, Pjetursson BE. A systematic review of the survival and complication rates of resin-bonded fixed dental prostheses after a mean observation period of at least 5 years. *Clin Oral Implants Res* 2017;28:1421—32.
10. Komine F, Blatz MB, Matsumura H. Current status of zirconia-based fixed restorations. *J Oral Sci* 2010;52:531—9.
11. Pjetursson BE, Sailer I, Makarov NA, Zwahlen M, Thoma DS. All-ceramic or metal-ceramic tooth-supported fixed dental prostheses (FDPs)? A systematic review of the survival and complication rates. Part II: multiple-unit FDPs. *Dent Mater* 2015;31:624—39.
12. Bakitian F, Papia E, Larsson C, Vult von Steyern P. Evaluation of stress distribution in tooth-supported fixed dental prostheses made of translucent zirconia with variations in framework designs: a three-dimensional finite element analysis. *J Prosthodont* 2020;29:315—22.
13. Lopez-Suarez C, Rodriguez V, Pelaez J, Agustin-Panadero R, Suarez MJ. Comparative fracture behavior of monolithic and veneered zirconia posterior fixed dental prostheses. *Dent Mater J* 2017;36:816—21.
14. Blatz MB, Alvarez M, Sawyer K, Brindis M. How to bond zirconia: the APC concept. *Comp Cont Educ Dent* 2016;37:611—8.
15. Zhang Y, Lawn BR. Novel zirconia materials in dentistry. *J Dent Res* 2018;97:140—7.
16. Al Hamad KQ, Obaidat II , Baba NZ. The effect of ceramic type and background color on shade reproducibility of all-ceramic restorations. *J Prosthodont* 2020;29:511—7.
17. Worni A, Katsoulis J, Kolgeci L, Worni M, Mericske-Stern R. Monolithic zirconia reconstructions supported by teeth and implants: 1- to 3-year results of a case series. *Quintessence Int* 2017;48:459—67.
18. Aung SSMP, Takagaki T, Lyann SK, et al. Effects of alumina-blasting pressure on the bonding to super/ultra-translucent zirconia. *Dent Mater* 2019;35:730—9.
19. Gulati J, Tabiat-Pour S, Watkins S, Banerjee A. Resin-bonded bridges – the problem or the solution? part 1: assessment and design. *Dent Update* 2016;43:506—21.
20. Ferrari M, Cagidiaco C, Bertelli E. Anatomic guide for reduction of enamel for acid-etched retainers. *J Prosthet Dent* 1987;58:106—10.
21. Paphangkorakit J, Osborn JW. The effect of pressure on a maximum incisal bite force in man. *Arch Oral Biol* 1997;42:11—7.
22. Koutayas SO, Kern M, Ferraresso F, Strub JR, Stub JR. Influence of design and mode of loading on the fracture strength of all-ceramic resin-bonded fixed partial dentures: an in vitro study in a dual-axis chewing simulator. *J Prosthet Dent* 2000;83:540—7.
23. Rosentritt M, Ries S, Kolbeck C, Westphal M, Richter EJ, Handel G. Fracture characteristics of anterior resin-bonded zirconia-fixed partial dentures. *Clin Oral Invest* 2009;13:453—7.
24. Bömicke W, Waldecker M, Krisam J, Rammelsberg P, Rues S. In vitro comparison of the load-bearing capacity of ceramic and metal-ceramic resin-bonded fixed dental prostheses in the posterior region. *J Prosthet Dent* 2018;119:89—96.
25. Kiliçarslan MA, Kedici PS, Küçükeşmen HC, Uludağ BC. In vitro fracture resistance of posterior metal-ceramic and all-ceramic inlay-retained resin-bonded fixed partial dentures. *J Prosthet Dent* 2004;92:365—70.
26. Northeast SE, van Noort R, Shaglouf AS. Tensile peel failure of resin-bonded Ni/Cr beams: an experimental and finite element study. *J Dent* 1994;22:252—6.
27. Durey KA, Nixon PJ, Robinson S, Chan MF. Resin bonded bridges: techniques for success. *Br Dent J* 2011;211:113—8.
28. Epprecht A, Zeltner M, Benic G, Özcan M. A strain gauge analysis comparing 4-unit veneered zirconium dioxide implant-borne fixed dental prosthesis on engaging and non-engaging abutments before and after torque application. *Clin Exp Dent Res* 2018;4:13—8.

29. Yamashita J, Shiozawa I, Takakuda K. A comparison of in vivo and in vitro strain with posterior fixed partial dentures. *J Prosthet Dent* 1997;77:250—5.
30. McLean JW, von Fraunhofer JA. The estimation of cement film thickness by an in vivo technique. *Br Dent J* 1971;131:107—11.
31. Matsuo S, Watari F, Ohata N. Fabrication of a functionally graded dental composite resin post and core by laser lithography and finite element analysis of its stress relaxation effect on tooth root. *Dent Mater J* 2001;20:257—74.
32. Sato T, Umehara K, Nakazawa A, Kosihara Y. Study on the enamel thickness of the anterior teeth of Japanese. *Adhes Dent* 1997;15:262—72.
33. Brokos Y, Stavridakis M, Bortolotto T, Krejci I. Evaluation of enamel thickness of upper anterior teeth in different age groups by dental cone beam computed tomography scan in vivo. *Int J Adv Case Rep* 2015;2:1396—409.
34. Nair A, Regish KM, Patil NP, Prithviraj DR. Evaluation of the effects of different groove length and thickness of the retainers on the retention of maxillary anterior base metal resin bonded retainers-an in vitro study. *J Clin Exp Dent* 2012;4:91—6.
35. Saad AA, Claffey N, Byrne D, Hussey D. Effects of groove placement on retention/resistance of maxillary anterior resin-bonded retainers. *J Prosthet Dent* 1995;74:133—9.
36. Onodera K, Sato T, Nomoto S, Miho O, Yotsuya M. Effect of connector design on fracture resistance of zirconia all-ceramic fixed partial dentures. *Bull Tokyo Dent Coll* 2011; 52:61—7.
37. Murase T, Nomoto S, Sato T, Shinya A, Koshihara T, Yasuda H. Effect of connector design on fracture resistance in all-ceramic fixed partial dentures for mandibular incisor region. *Bull Tokyo Dent Coll* 2014;55:149—55.